Large-area laser nano-texturing with user-defined patterns

2009 J. Micromech. Microeng. 19 054002

(http://iopscience.iop.org/0960-1317/19/5/054002)

J. Micromech. Microeng. **19** (2009) 054002 (6pp) doi:10.1088/0960-1317/19/5/054002

Large-area laser nano-texturing with user-defined patterns

L Li[1,4], W Guo[1,2], Z B Wang[1], Z Liu[2], D Whitehead[1] and B Luk'yanchuk[3]

[1] Laser Processing Research Centre, School of Mechanical, Aerospace and Civil Engineering, The University of Manchester, Sackville Street, Manchester M60 1QD, UK
[2] Corrosion and Protection Centre, School of Materials, The University of Manchester, Sackville Street, Manchester, M60 1QD, UK
[3] Data Storage Institute, DSI Building, 5 Engineering Drive 1, Singapore 117608

E-mail: Lin.li@manchester.ac.uk

Received 24 August 2008, in final form 2 December 2008
Published 14 April 2009
Online at stacks.iop.org/JMM/19/054002

Abstract
Writing nano-sized features less than the diffraction limit of the lasers efficiently over a large area requires special technology development. This paper reports the use of a self-assembled particle lens array with near-field enhancement effect to write millions of nano-sized user-defined features, e.g. English letters, lines, curves, simultaneously by angular beam scanning. About a 5 mm × 5 mm area can be written with a single shot of a laser beam or few scans for up to 100 million identical features of nano or sub-micro scales. With the help of certain environmental conditions, such as the use of a suitable chemical solution in conjunction with the particle lens array, the characteristic of the features produced can be further controlled, including the generation of reversed (e.g. pits become hills and grooves become walls) features of laser-written patterns. The technical challenges, experimental findings and theoretical analysis/simulation are presented.

(Some figures in this article are in colour only in the electronic version)

1. Introduction

As electrical–mechanical and optical devices get smaller, the need to consider surface tomography becomes more important. Tribological characteristics, optical absorption, wettability, cell interaction with surfaces and even aerodynamic and hydrodynamic properties of micro-devices are dependent on surface characteristics and surface textures. To tailor surface characteristics for specific properties through texturing requires high efficiency micro/nano-fabrication technology. Under normal conditions using far-field optics, the smallest feature size for laser patterning on surfaces is diffraction limited to the laser beam wavelength for direct beams and to half of the laser wavelength if an interference technique is used. These are generally of sub-micrometres (>100 nm), unless the laser wavelength is in deep UV where optics become expensive and easy to get damaged. Electron beams and focused ion beams are capable of writing features with resolutions down to 10 nm. These techniques, however, are not suitable for large-area (>1 cm^2) surface texturing due to the long time required when features are written in series. Recently, near-field optics (NFO) has attracted great attention in order to extend laser fabrication resolution to below the diffraction limit. NFO deals with optical phenomena where an evanescence wave or plasmonic field enhancement becomes significant and the sizes of the scattering objects in the laser beam path are of the order of a wavelength or smaller [1]. Several near-field patterning techniques exist: laser-integrated scanning near-field optical microscopy (SNOM) [2–4], laser-assisted AFM/STM-tip patterning [5–7], micro-lens arrays (MLA) [8] and contacting particle-lens array (CPLA) [9–11]. These techniques have demonstrated the capability of creating features on a surface smaller than the diffraction limits of the lasers used. Furthermore, MLA and CPLA are parallel processing techniques that can allow many identical features to be produced simultaneously.

One of the common problems of most near-field optical systems for surface patterning is that the processing optics are very close to the target surface giving opportunities

[4] Corresponding author.

for contamination and damage by the surface debris generated during the processing of materials when melting or vaporization is involved. In addition, most of the NFO techniques require precise control of the distance and orientation between the processing optic/tip and the target surface. Compared with other near-field laser patterning techniques, CPLA has the advantages of low cost, contact optical system (thus, no precise distance control is required and can follow curved surfaces), simple set-up and fast speed. CPLA is carried out by means of two-dimensional lattices of optically transparent micro-spheres that are formed by self-assembly. Due to the multiple internal reflections occurring inside the spherical cavities of particles, evanescent waves are generated around the particle surfaces which cause interferences with the incident beam and produce higher energy localization on the surface below the particle [12]. However, the existing CPLA technique has a limitation of only allowing a single shot by the laser, and most of the particles are removed following a single laser pulse exposure due to the thermal deformation force and ablative force exceeding the particle–substrate adhesion force [13]. The disappearance of the particle lens makes it impossible to fabricate a complex patterns array other than shallow dents or a dots array. To keep particles on the surface for repeatable patterning, an angular laser beam scanning (ALBS) technique was introduced by the authors [14]. This paper further extends this work to allow more complex patterns at nano-scales to be fabricated over a larger area. Furthermore, the introduction of a chemical solution during laser fabrication has demonstrated to allow more complicated geometries to be fabricated at high efficiency.

2. Experimental procedures

A KrF excimer laser (GSI-Lumonic IPEX848) was used as the light source (wavelength $\lambda = 248$ nm, pulse duration $\tau = 15$ ns and repetition rates from 1 to 10 Hz, non-polarized). The laser beam spot size is around 18 mm $\times$ 10 mm in a rectangular shape. The beam was directly incident on the sample surface without focusing. Two types of experimental materials for nano-texturing were used. For the dry processing experiment, the target material to be textured was a 20 nm thick, semi-conductive $Sb_{70}Te_{30}$ thin film (refractive index $n = 1.80 + 2.07i$) coated on a polycarbonate substrate ($n = 1.57 + 0.12i$). A close-packed monolayer of SiO_2 spheres ($r = 500$ nm) was directly formed onto the thin film surface over an area of 5 $\times$ 5 mm^2 by the self-assembling process, which was carried out by drop coating of the colloidal particles solution onto the cleaned, hydrophilic sample surface and leaving it to dry in the air environment. The spheres are a commercially available suspension from Duke Scientific Cooperation. The threshold fluence of the thin film ablation was about 20 mJ cm^{-2}. The laser energies used to ablate the materials were 100–300 mJ/pulse. As shown in figure 1, the laser beam was scanned in the *YZ* plane with an incident angle θ. The intensity peaks on the substrate are shifted away from the contacting point, which means that the ablative forces do not react with micro-spheres. Therefore, the spheres can

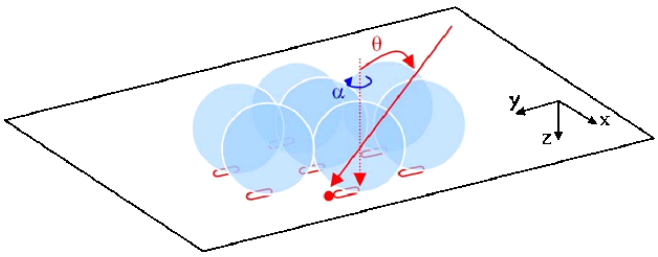

Figure 1. Schematic diagram of the experimental configuration for direct laser writing of nano-line arrays on the substrate surface.

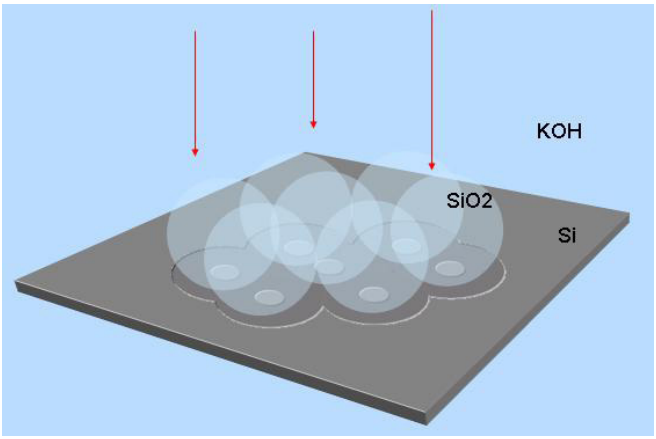

Figure 2. Schematic of wet chemical-assisted laser nano-patterning using a particle lens array.

be kept on surface after processing. As particles remained on the surface, multiple shots of the laser beam are able to be applied. To form a continuous line, a single laser pulse was used for every small angle ($\pi/36$) scanned through the spheres. The scanning range was controlled within ($-\pi/4$, $\pi/4$). The normal incident beam was set to be the final shot of the process to avoid removing the particles during the scanning. As the laser intensity on the target at various scanning angles is different [14], the laser beam intensity was adjusted to enable uniform feature sizes.

For the wet chemical-assisted CPLA processing technique, the target material was an n-type single crystal Si (1 0 0) wafer with a resistance of 3–5 Ω cm^{-1}. A close-packed monolayer of SiO_2 spheres ($r = 250$ nm) was directly formed onto the Si surface by self-assembly, as shown in figure 2. About 10^8 spheres can be formed in an area of 0.5 m^2.

n-type silicon can be etched using a 30%wt KOH solution. The reaction between Si and OH is weak at room temperatures. However, at elevated temperatures effected by the laser beam and the CPLA, an accelerated chemical reaction would occur:

$$Si + 2H_2O + 2OH^- \rightarrow Si(OH)_2(O^-)_2 + 2H_2. \qquad (1)$$

The samples were then characterized by field emission gun scanning electron microscopy (FEG-SEM; Philips XL32) and atomic force microscopy (AFM; Vecco CP2).

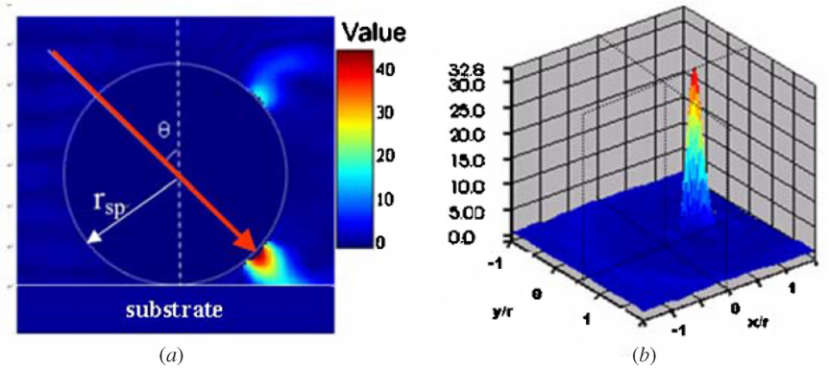

(*a*) (*b*)

Figure 3. Calculated Poynting intensity distribution S_z for $\lambda = 248$ nm radiation with an incident angle ($\theta = 30^\circ$) under a SiO_2 sphere ($n = 1.51$) of radius ($r = 500$ nm) on the SbTe substrate ($n = 1.80$, $k = 2.07$). (*a*) A 2D view and (*b*) a 3D view.

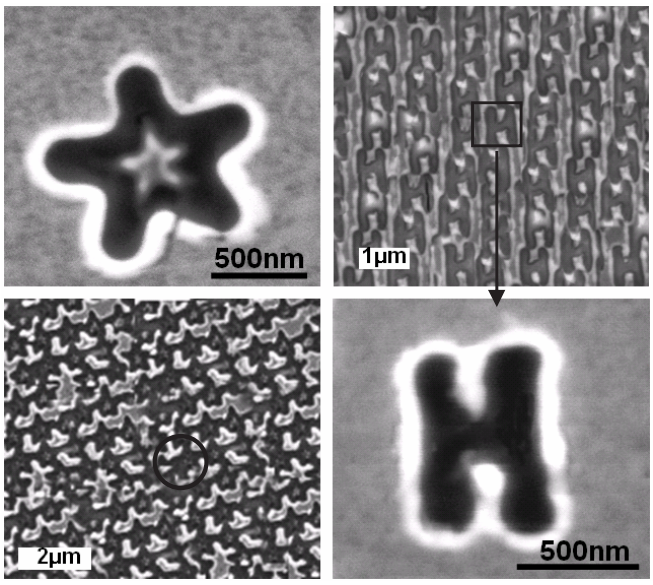

(*a*) (*b*)

Figure 4. SEM images of star-shape arrays (*a*) and H-shape arrays (*b*) produced by scanning beams with designed angles. Six million of the 'identical' patterns were produced simultaneously.

3. Results

3.1. Angular laser beam scanning with a micro-lens array for complex user-defined nano-patterns

The optical near fields around the particles were simulated by a rigorous analytical particle on surface (POS) model, shown in figure 3. The electromagnetic modes, including the evanescent modes, were taken into account in the model. Detailed information on the models can be found in [15, 16]. The peak enhancement was about 32.8 times and would decay rapidly with the increase of angle θ.

The angle θ controls the position of the intensity peak point in the radial direction, while the angle α moves it in the circumferential direction. By turning α with a small angle ($\pi/36$) each time and scanning θ at a particular angle, user-defined patterns can be easily fabricated, as illustrated in figure 4. The processing volume of each hot spot is limited locally and well away from the particle/substrate contact zone. Thus, the removed substrate materials have no clear experimental impact on the particle position for subsequent laser shots. Both star-shape and H-shape features are about 1 μm in the X or Y dimension and are 20 nm deep. A very small star island (less than 300 nm) can be identified within the stars with the tip feature size less than 30 nm. Tens of millions of these features were generated simultaneously by 72 laser shots at different locations.

3.2. Wet chemical-assisted laser particle lens array nano-patterning

Two examples of wet chemical laser-assisted particle lens array textured n-type silicon in an aqueous KOH solution are shown in figure 5 for processing by using two different laser fluences. At a relatively low laser fluence (0.59 mJ cm^{-2}), a ring-shaped structure was produced with the central island nano-bump size around 50 nm in diameter, whilst at a higher fluence (0.73 mJ cm^{-2}), dents were produced with an average diameter of 200 nm. The holes are not perfectly round in shape, and some of the hole edges are broken and linked together with neighbouring holes. The main reason could be the fluctuation of the optical near fields due to the additional scattering by H_2 bubbles (as in equation (1)) as well as the possible perturbation of the stationary liquid solution during the process.

Figure 6 shows the dimensional measurement of the two types of structure shown in figure 5 using atomic force microscopy compared to theoretically determined optical energy intensity field distribution in the chemical solution. This confirms the dimensions mentioned above for the features created with a typical depth of 20 nm. At low fluences, the surface structure produced follow approximately the energy density field profiles, whilst at high fluence, the feature shape is different from that of the energy field but with a similar width as the energy field.

The shape of the features can be further modified by etching the processed samples in a warm KOH solution (30 wt%, 40 °C, 2 min). The etch rate was approximately 0.1 μm min^{-1}. Figure 7 shows the results of further chemical etching after the above surface patterning. It can be seen that the geometry of features was changed from concave to convex. This change was believed to be caused by the formation of local oxide layers in the laser-machined region

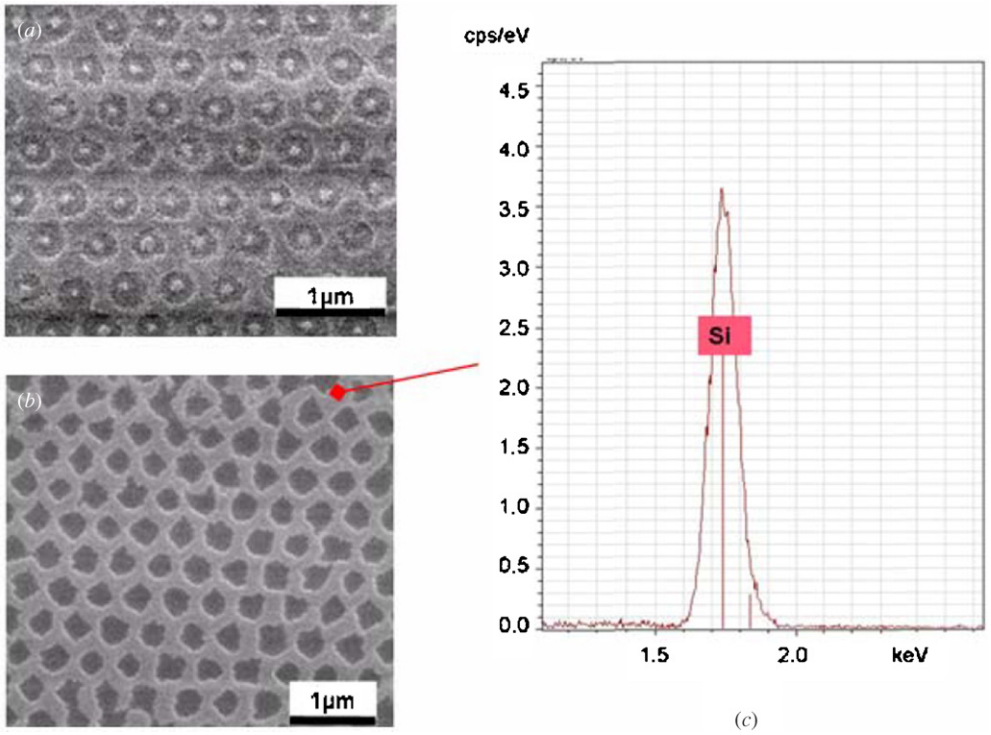

Figure 5. SEM image structures produced with the wet chemical-assisted laser particle lens array surface texturing in 30% KOH, with (*a*) a laser fluence of 0.59 mJ cm^{-2}, (*b*) a laser fluence of 0.73 mJ cm^{-2} and (*c*) the EDX element analysis on the top surface of the sample.

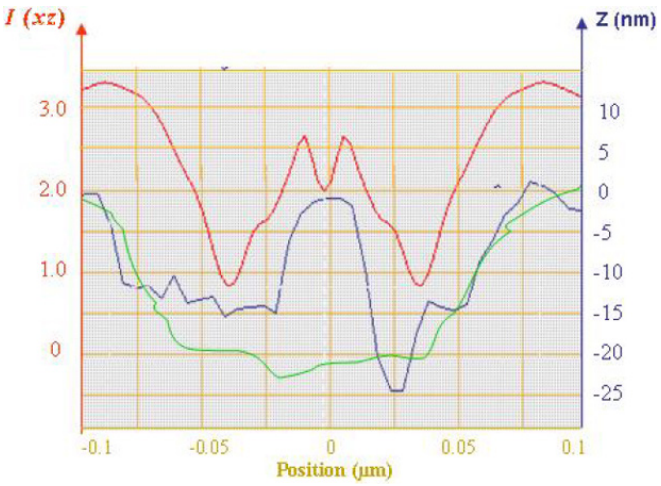

Figure 6. Calculated energy intensity in the *XZ* plane (upper, red line) and the AFM profile of the ring-shaped structure in figure 5(*a*) (middle, blue line) and dent shapes in figure 5(*b*) (lower, green line).

(EDX measurement showing oxide formation in figure 5 on the top of nano-bumps) that would prevent chemical etching. A possible chemical process during the post-process etching can be shown as follows:

$$\mathrm{Si(OH)_2(O^-)_2} \rightarrow \mathrm{SiO_2} + 2\mathrm{OH^-}. \qquad (2)$$

Figure 8 shows the AFM profile of arrays of bump-shape nano-structures fabricated by the proposed technique. The average nano-bump size was 250 nm in width and 40–60 nm in height.

4. Discussion

Nano-texturing over a large area requires parallel processing techniques. The work here demonstrated the use of the near-field effect of small transparent particles to realize this by splitting a single laser beam into millions of beams that are able to produce features below the diffraction limit of the lasers. By firing the laser beam at various angles, not only the particles can stay for multiple shots (not possible before), but also various user-defined patterns can be produced (also not previously available). In particular, the spacing between the patterns is no longer limited by the transparent particle size using this new technique and the depth of patterns could be increased by repeated laser radiation. This represents a useful advancement of the near-field parallel nano-patterning technique. The patterns can be reversed through the use of chemical-assisted patterning and further etching as described here. The two techniques therefore would be able to provide means to produce user-defined textured surfaces on small objects, such as MEMs (for improved tribological characteristics) and LEDs (for improved emission efficiency), and medium-sized objects, such as moulds and dies, that may potentially be used to produce textured surfaces (for wettabilitiy control, optical reflectivity control, etc) on plastic materials through injection moulding. One of the issues that would need to be considered carefully is the uniformity of self-assembled transparent particles. Monolayer, uniform distribution of transparent particles is a key requirement. This is not always readily achievable. Careful work piece preparation would be needed. The minimum particle size is

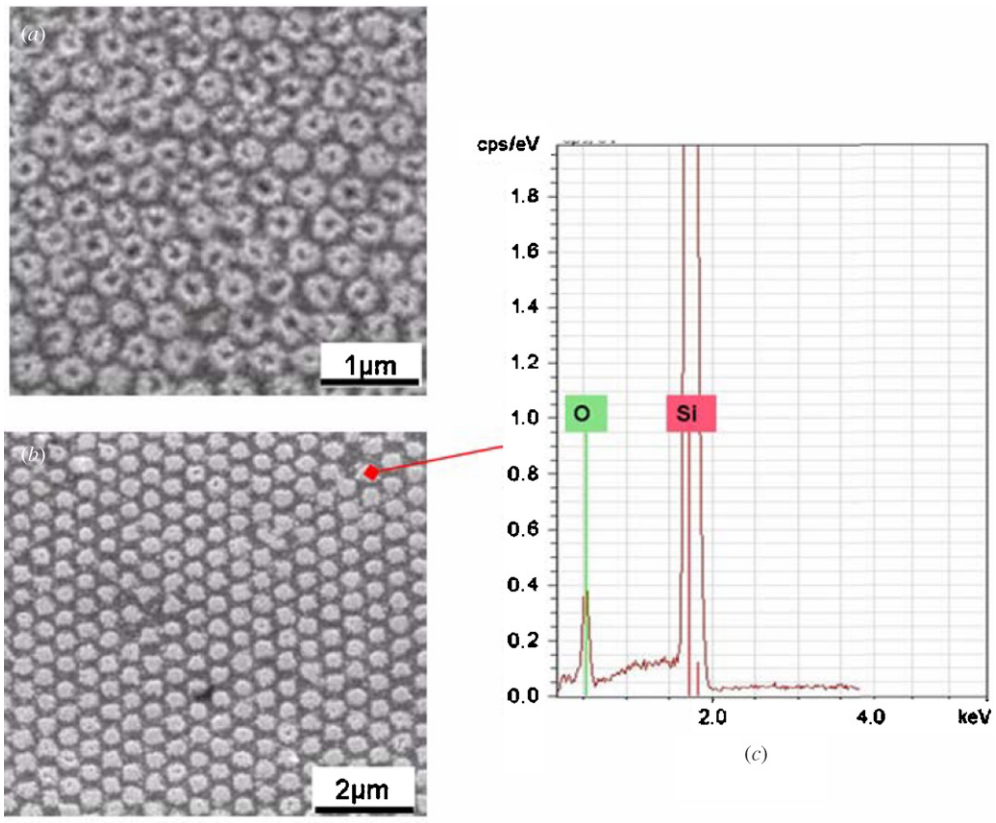

Figure 7. SEM images of structures produced with further wet chemical etching in warm 30% KOH for 2 min, corresponding to figures 5(*a*) and (*b*), separately, with completely reversed surface structures. (*c*) EDX element analysis of the surface of nano-bumps formed.

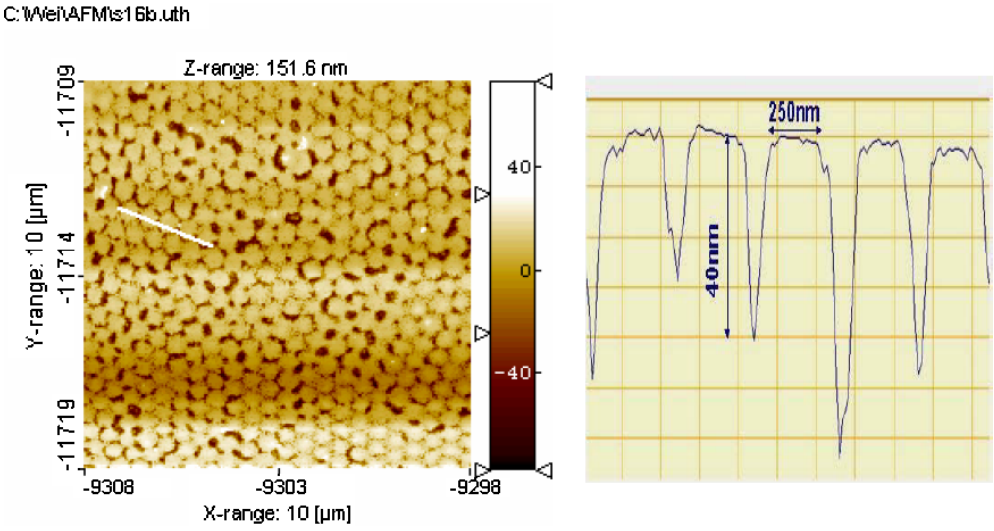

Figure 8. AFM profile of ordered arrays of nano-bump structures with 250 nm in width and 40–60 nm in height.

currently limited to 0.5 μm. An advantage of the technique is that curved surfaces could be potentially patterned.

Micro-lens array near-field parallel patterning would be a better technique compared to the particle lens array technique. The uniformity of patterns produced by the micro-lens array is excellent if the lens array can be made absolutely parallel to the surface of the work piece. One specific requirement of the micro-lens array is the precise control of the distance (e.g. a few micrometres) between the lens arrays and the work piece for each lens. This is difficult if the surface of the work piece is not flat. Also, possible damages by the debris from the work piece could reduce the life of the micro-lens arrays. Therefore, a particle lens array would provide an alternative, economic means for large-area nano-patterning/texturing.

5. Conclusions

A new laser-based nano-texturing technique has been demonstrated by the use of a self-assembled mono-layer particle lens array and angular incident laser beams and the

use of a chemical solution. The method has shown to produce complex user-defined nano-scale structures over a large area with structure sizes below the diffraction limit of the laser beams. Several million identical nano-patterns have been produced simultaneously.

Acknowledgments

The authors acknowledge the support of the work by Northwest Development Agency (grant number: N0003200), through the Northwest Laser Engineering Consortium, a collaboration between the Universities of Manchester and Liverpool.

References

[1] Girard C and Dereux A 1996 Near-field optics theories *Rep. Prog. Phys.* **59** 657–99
[2] Betzig E and Trautman J K 1992 Near-field optics—microscopy, spectroscopy, and surface modification beyond the diffraction limit *Science* **257** 189–95
[3] Riehn R, Charas A, Morgado J and Cacialli F 2003 Near-field optical lithography of a conjugated polymer *Appl. Phys. Lett.* **82** 526–8
[4] Wysocki G, Heitz J and Bauerle D 2004 Near-field optical nanopatterning of crystalline silicon *Appl. Phys. Lett.* **84** 2025–7
[5] Boneberg J, Münzer H J, Tresp M, Ochmann M and Leiderer P 1998 The mechanism of nanostructuring upon nanosecond laser irradiation of a STM tip *Appl. Phys.* A **67** 381–4
[6] Dickmann K, Jersch J and Demming F 1997 Focusing of laser radiation in the near-field of a tip (FOLANT) for applications in nanostructuring *Surf. Interface Anal.* **25** 500–4
[7] Jersch J and Dickmann K 1996 Nanostructure fabrication using laser field enhancement in the near field of a scanning tunneling microscope tip *Appl. Phys. Lett.* **68** 868–70
[8] Kato J I, Takeyasu N and Adachi Y 2005 Multiple-spot parallel processing for laser micronanofabrication *Appl. Phys. Lett.* **86** 044102
[9] Arias-Gonzlez J R and Nieto-Vesperinas M 2000 Near-field distributions of resonant modes in small dielectric objects on flat surf aces *Opt. Lett.* **25** 782–4
[10] Denk R, Piglmayer K and Bauerle D 2002 Laser-induced nanopatterning of PET using a-SiO_2 microspheres *Appl. Phys.* A **74** 825–6
[11] Brodoceanu D, Landstrom L and Bauerle D 2007 Laser-induced nanopatterning of silicon with colloidal monolayers *Appl. Phys.* A **86** 313–4
[12] Hong M H, Huang S M, Luk'yanchuk B S and Chong T C 2003 Laser assisted surface nanopatterning *Sensors Actuators* A **108** 69–74
[13] Zheng Y W, Luk'yanchuk B S, Lu Y F, Song W D and Mai Z H 2001 Dry laser cleaning of particles from solid substrates: experiments and theory *J. Appl. Phys.* **90** 2135–42
[14] Guo W, Wang Z B, Li L, Whitehead D, Luk'yanchuk B S and Liu Z 2007 Near-field laser parallel nanofabrication of arbitrary-shaped patterns *Appl. Phys. Lett.* **90** 243101
[15] Wang Z B, Hong M H, Luk'yanchuk B S, Lin Y, Wang Q F and Chong T C 2004 Angle effect in laser nanopatterning with particle-mask *J. Appl. Phys.* **96** 6845–50
[16] Wang Z B, Guo W, Luk'yanchuk B S, Whitehead D J, Li L and Liu Z 2008 Optical near-field interaction between neighboring micro/nano-particles *J. Laser Micro/Nanoeng.* **3** 14–8